

DirectSwap: Mask-Free Cross-Identity Training and Benchmarking for Expression-Consistent Video Head Swapping

Yanan Wang^{1,2} Shengcai Liao^{2*} Panwen Hu¹ Xin Li³ Fan Yang³ Xiaodan Liang^{1,4}

¹MBZUAI ²UAEU ³AIQ ⁴SYSU

Abstract

Video head swapping aims to replace the entire head of a video subject, including facial identity, head shape, and hairstyle, with that of a reference image, while preserving the target body, background, and motion dynamics. Due to the lack of ground-truth paired swapping data, prior methods typically train on cross-frame pairs of the same person within a video and rely on mask-based inpainting to mitigate identity leakage. Beyond potential boundary artifacts, this paradigm struggles to recover essential cues occluded by the mask, such as facial pose, expressions, and motion dynamics. To address these issues, we prompt a video editing model to synthesize new heads for existing videos as fake swapping inputs, while maintaining frame-synchronized facial poses and expressions. This yields HeadSwapBench, the first cross-identity paired dataset for video head swapping, which supports both training (8,066 videos) and benchmarking (500 videos) with genuine outputs. Leveraging this paired supervision, we propose DirectSwap, a mask-free, direct video head-swapping framework that extends an image U-Net into a video diffusion model with a motion module and conditioning inputs. Furthermore, we introduce the Motion- and Expression-Aware Reconstruction (MEAR) loss, which reweights the diffusion loss per pixel using frame-difference magnitudes and facial-landmark proximity, thereby enhancing cross-frame coherence in motion and expressions. Extensive experiments demonstrate that DirectSwap achieves state-of-the-art visual quality, identity fidelity, and motion and expression consistency across diverse in-the-wild video scenes. We will release the source code and the HeadSwapBench dataset to facilitate future research.

1. Introduction

Video head swapping extends beyond traditional face swapping [1, 4, 7, 18, 42] and image-based head swapping [17, 27, 34] by reconstructing entire head region, including hair,

ears, jawline, etc., and re-anchoring it within the target’s body and motion field. This reframing transforms a localized appearance edit into a physically grounded video generation problem, in which identity, geometry, and dynamics must be modeled as a unified process. High-fidelity head synthesis now underpins pipelines for digital humans and virtual avatars, cinematic post-production and relighting, telepresence, and privacy-preserving or personalized media creation. In these scenarios, realism is judged not only by facial expression but by the seamless continuity of hairstyle, silhouette, and head-body interaction through motion. Heads exhibit nonrigid volumetric structure and intricate hair-body couplings that vary with pose, illumination, occlusion, and compression. Capturing these effects requires more than frame-wise feature alignment: it demands understanding how head identity evolves over time.

Despite this broad utility and active research in face swapping [1, 4, 7, 18, 42] and image-based head swapping [17, 27, 34], video head swapping remains largely underexplored [14]. The task unifies the most difficult aspects of identity preservation, physical head-scene fusion, and temporal coherence: hair, silhouette, and craniofacial contours must remain stable across large pose and expression changes, while the synthesized head must integrate naturally with the body and background, including transferring illumination, handling self-occlusion, and maintaining neck-torso continuity, without brittle, hand-crafted masks or matting. Progress has been further constrained by the lack of *cross-identity paired* swapping supervision that enables explicit identity-motion learning, and by fragmented evaluation protocols that fail to jointly assess identity fidelity, hairstyle accuracy, and sequence-level stability.

Due to the lack of ground-truth paired swapping data, prior methods [14, 17, 27, 34] typically train on cross-frame pairs of the same person within a video and rely on *mask-based inpainting paradigm* to mitigate identity leakage. They explicitly segment or crop the head region, replacing with mask, and formulate generation as conditional inpainting, guided by identity embeddings, background context, and pose or landmark cues. The model first reconstructs the

*Corresponding author.



Figure 1. **Qualitative results on zero-shot video head swapping.** Given a reference head and a driving video (Vd), our method synthesizes the entire head while preserving the background, body, and expression dynamics. **Top:** comparison with existing methods on HeadSwapBench with ground-truth videos (V_a). **Bottom:** our temporally consistent results across video frames.

masked background and then synthesizes the head within the designated area. While this setup offers local controllability, it enforces an artificial spatial boundary between the head and the surrounding scene, disrupting geometric and photometric continuity at the hairline, neck, and shoulder transitions. Furthermore, beyond potential boundary artifacts, this paradigm struggles to recover essential cues occluded by the mask, such as facial pose, expressions, and motion dynamics. As a result, it’s challenging for existing methods to generate identity-preserved (including head shape and hair style), and motion-/expression-consistent head swapping videos, as observed in Fig. 1.

To overcome these limitations, we create HeadSwapBench, the first large-scale *cross-identity paired* dataset for video head swapping, which supports both training and benchmarking with genuine outputs. The HeadSwapBench dataset contains 8,066 paired training videos and 500 paired test videos for benchmarking. As shown in Fig. 1, each video pair contains a fake driven video (V_d) and a real-world ground-truth video (V_a) as desired output. Particularly, the V_d - V_a pair is frame synchronized in background, subject body, head poses, and facial expressions etc., differing only in two different head identities. Specifically, we prompt a

video editing model [15] to synthesize new heads for existing videos (V_a), resulting in fake head-swapped driven video (V_d), while maintaining frame-synchronized facial poses and expressions. To ensure data reliability, we further apply automated filtering to remove low-quality, misaligned, or photometrically inconsistent sequences, yielding a clean and temporally stable corpus that supports robust learning of head swapping through motion.

Building on this data regime, we propose DirectSwap, a mask-free, direct video head-swapping framework based on diffusion model. Instead of restricting synthesis to masked regions, the proposed DirectSwap method learns video head swapping through direct supervision from frame-synchronized, cross-identity motion pairs enabled by HeadSwapBench. Specifically, the proposed method extends an image U-Net into a video diffusion model with a motion module and conditioning inputs, where the reference head and driving video are encoded into two latent canvases whose features are jointly fused and denoised within a unified diffusion process. This design allows identity and motion cues to be continuously aligned, enabling physically coherent head synthesis under dynamic conditions. Furthermore, we introduce the Motion- and Expression-Aware Re-

construction (MEAR) loss, which reweights the diffusion loss per pixel using frame-difference magnitudes and facial-landmark proximity, thereby enhancing cross-frame coherence in motion and expressions. Together, HeadSwapBench and DirectSwap form a new paradigm for mask-free direct video head swapping with smooth identity–motion generation that achieves temporally stable, geometrically consistent, and photorealistic results. Overall, our **contributions** are threefold:

- We redefine video head swapping as a continuous identity–motion generation problem, moving beyond the conventional mask-based inpainting paradigm that isolates head synthesis within static masks. This new formulation emphasizes physical coherence across geometry, motion, and appearance.
- We create **HeadSwapBench**, a cross-identity paired video head swapping dataset that provides explicit supervision of head swapping across motion, enabling both training and evaluation of the mask-free video head swapping task.
- We present **DirectSwap**, a mask-free, direct video head-swapping framework via an enhanced video diffusion model, equipped with a **Motion- and Expression-Aware Reconstruction (MEAR)** loss. Extensive experiments demonstrate that DirectSwap achieves state-of-the-art visual quality, identity fidelity, and motion and expression consistency across diverse in-the-wild video scenes.

2. Related Work

Image Inpainting. Image inpainting aims to fill missing or occluded regions so that the completed image remains photorealistic and semantically plausible. Early deep methods are mostly GAN-based: Context Encoders [25] and follow-ups [12, 21, 24] use encoder–decoder architectures with adversarial losses to hallucinate large holes, but often fail to maintain semantics when the missing region intersects salient objects or complex layouts. Diffusion-based methods overcome many of these issues by performing iterative masked denoising. RePaint [23] and subsequent score- and latent-diffusion approaches [5, 29, 30] leverage large pretrained models to reconstruct fine details and long-range structure, setting the current state of the art in semantic- and context-aware inpainting—yet they still treat the edited region as a local mask, rather than explicitly modeling object identity and motion.

Head Swapping Methods. Most face-swapping methods [1, 18, 42] operate on cropped facial regions, keeping hairstyle and head shape fixed. This simplifies alignment but limits realism when the head silhouette or hair texture differs across identities. HeSer [27] first transfers the full head using a two-stage GAN pipeline for pose alignment and background blending, while HS-Diffusion [34] incorporates diffusion priors with semantic calibration and

neck alignment. HID [17] extends this direction to zero-shot transfer with IOMask for unconstrained identity swapping. More recently, SwapAnyHead [14] introduces a controllable diffusion-based framework that enhances hair and expression consistency through shape-agnostic masks and landmark retargeting. However, these methods remain *mask-dependent*, confining synthesis to predefined regions without modeling temporal transport or head–body coupling. They rely on unpaired supervision and treat each frame independently, which limits geometric and temporal coherence. Our DirectSwap, trained on the paired HeadSwapBench benchmark, learns explicit identity–motion correspondences, enabling temporally consistent, geometry-aware head generation.

Video Diffusion Models. Diffusion models have been extended from images to videos with promising temporal quality. Video Diffusion Models [11] use 3D U-Nets to capture joint spatiotemporal dependencies, while later works [2, 8, 39] adapt image diffusion backbones with motion priors or temporal layers for zero-shot text- or image-conditioned video generation. Following AnimateDiff [8], one can attach a lightweight motion module to an image diffusion model to obtain temporally correlated samples.

3. HeadSwapBench

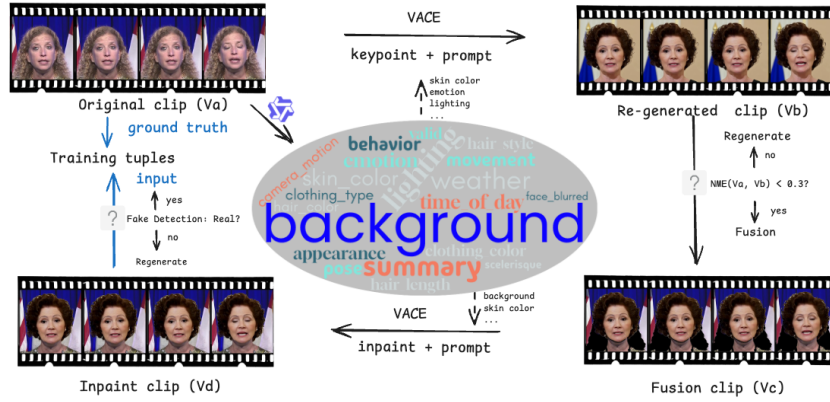
Current benchmarks for head manipulation provide only unpaired talking-head videos or self-paired frames, making it difficult to learn and evaluate identity transport through motion. To fill this gap, we construct **HeadSwapBench**, a paired video benchmark tailored to identity-preserving head swapping. Each sample consists of a synthetic input video whose background, body, motion and expression are inherited from a real clip, and a ground-truth video that shows how the same sequence should look with the target head identity, enabling fully supervised diffusion training and full-reference evaluation.

3.1. Data Generation Pipeline

Obtaining true ground truth for transferring a head across different bodies is inherently difficult: the same motion and scene rarely exist for two distinct identities. Prior work often samples frames of the *same* person from a single video and trains with masked targets to avoid trivial copying; mask misalignment, however, deforms the subject and destabilizes training (see Fig. 5). Other methods [15] mask large background regions and require the model to hallucinate both subject and context, which breaks motion continuity and temporal coherence (see Fig. 4). HeadSwapBench is designed to avoid both issues. The pipeline in Fig. 2 transforms unpaired talking-head videos into paired head-swapping data while keeping backgrounds and motion real.

Original Clips as Ground Truth. We start from single-person clips in HDTF [41] and VFHQ [37]; each original

Dataset Generation Pipeline



Training Tuples



Figure 2. **HeadSwapBench dataset generation and training pairs.** Left: pipeline of prompting VACE [15] to synthesize new heads for existing videos (V_a), resulting in fake head-swapped driven video (V_d), while maintaining frame-synchronized facial poses and expressions. Right: example training pairs where input V_d and ground truth V_a share background and motion but differ in identity. See details in Sec. 3.

clip is denoted V_a and is treated as the ground-truth head-swapped sequence. V_a provides the background, body, and motion that the swapped head must follow.

Attribute and Motion Extraction. For each V_a , a vision-language model (Qwen2.5-VL-72B-Instruct [32]) extracts high-level attributes of the video, including background layout, lighting, skin tone, etc. In parallel, PIP-Net [16] detects facial landmarks frame by frame, capturing pose and expression. These attributes and landmarks together form the control signal for the later video editing.

Video Editing by VACE. We feed the facial landmarks and VLM-derived attributes into VACE [15] to synthesize a new video sequence V_b whose motion is driven by the detected landmarks and whose appearance is conditioned on textual attributes (see **Supplementary Material A.1**). To verify motion transfer, we get PIPNet landmarks on V_a and V_b and compute the normalized mean error (NME) [3] between facial landmarks. If the NME exceeds a dataset-specific threshold (empirically set 0.3), indicating misalignment, we discard V_b and regenerate until the motion matches V_a .

Head Fusion and Background-Aware Inpainting. Given a well-aligned V_b , we extract head regions in V_a and V_b using the MediaPipe segmentation model [22]. The motion-preserved generated new head from V_b is pasted onto original background of V_a , yielding a synthetic fusion V_c . Because VACE preserves geometric alignment, the head can be composited with minimal distortion. Residual gaps or artifacts around the hairline and neck are then inpainted using VACE with background-aware textual descriptions, producing final synthetic video V_d that shares the scene, body, and motion of V_a but presents a different head identity.

Automatic Realism Filtering and Training Tuples. To

further ensure realism, we pass V_d through Xception-Net [26] trained for deepfake detection. Videos whose predicted “real” probability falls below a threshold (empirically set to 0.7) are discarded and regenerated from earlier stages of the pipeline. After filtering, HeadSwapBench contains 8,566 visually plausible and temporally stable clips. Each training tuple comprises: (i) the synthetic input video V_d , (ii) a source identity image I_b sampled from V_a for identity conditioning, and (iii) the original video V_a providing ground-truth supervision. V_d and V_a share background and motion while differing in head identity, compelling the model to modify identity alone. This design makes HeadSwapBench not only a high-quality benchmark but also a scalable data-generation framework for future large-scale head synthesis research.

3.2. Evaluation Protocol and Metrics

Evaluating video head swapping is challenging without paired supervision. HeadSwapBench provides, for each sample, a synthetic input V_d and a ground-truth video V_a , enabling evaluation directly against the *desired* head-swapped result rather than the input itself. The test set comprises 500 identity-disjoint clips, manually curated for perceptual quality. In a user study of 200 users, over 90% of the V_d videos were judged as real, confirming the reliability of V_d for full-reference evaluation. Unless otherwise stated, frame-level metrics are averaged over time, and FID is computed over all test frames. We assess four core performance dimensions: identity similarity, pose and expression consistency, frame-wise fidelity, and temporal stability.

Identity Similarity. Identity preservation is quantified by the cosine similarity of ArcFace embeddings [6] between

the generated video and V_a . Comparing against V_a , rather than the reference image, eliminates pose and expression bias, providing a direct measure of how faithfully the target identity is maintained.

Pose and Expression Consistency. HeadSwapBench evaluates how accurate models reproduce the target’s motion and facial dynamics. SynergyNet [36] estimates Euler angles and facial landmarks from both videos; pose accuracy is measured by mean absolute error (MAE) over angles, and expression consistency by normalized mean error (NME) over landmarks. Lower MAE and NME indicate closer alignment between generated and ground-truth motion.

Frame-Wise Fidelity: SSIM, PSNR, LPIPS, and FID. Per-frame image quality is evaluated using SSIM [35], PSNR [13], LPIPS [40], and FID [10], comparing generated frames with V_a . LPIPS is computed with AlexNet [19], and FID with Inception-V3 [31]. These metrics jointly capture perceptual realism, structural integrity, and data fidelity under matched motion and background.

Temporal Stability: tLPIPS. Temporal coherence is measured by tLPIPS [28], which computes perceptual variation across adjacent frames. Lower tLPIPS values correspond to smoother motion, fewer flickering artifacts, and more consistent blend of the head with the body and context.

4. Methodology

We propose a fully supervised and mask-free method for video head swapping, trained on paired sequences from HeadSwapBench. Unlike conventional approaches that depend on handcrafted masks, our method learns head transformation as a *continuous generative process* in latent space. Each paired sample (V_d, V_a) shares identical motion and background but differs in identity, establishing explicit alignment between appearance and dynamics. Leveraging this property, our framework DirectSwap models identity transfer as a geometry-aware mapping across two latent domains. It comprises two main components: (1) a Dual-Canvas Conditioning scheme that preserves motion–identity alignment within the latent geometry, and (2) a Motion- and Expression-Aware Reconstruction (MEAR) loss that emphasizes motion and expressive to enhance perceptual fidelity and temporal coherence.

4.1. Dual-Canvas Conditioning

The goal of head swapping is to transfer a source identity onto a target video while preserving the original background, body, and motion. Conventional inpainting methods rely on predefined masks that localize edits but disrupt geometric continuity and limit contextual understanding. We reformulate the task as a *continuous generative process* in latent space, where identity and motion interact through spatially adjacent domains.

Let the encoded target video be $Z_t \in \mathbb{R}^{B \times C \times F \times H \times W}$ and the reference head image be $Z_r \in \mathbb{R}^{B \times C \times H \times W}$. We replicate Z_r across frame and concatenate it with Z_t along the width dimension:

$$Z_{\text{cond}} = \text{Concat}_W(Z_t, \text{Repeat}_F(Z_r)) \in \mathbb{R}^{B \times C \times F \times H \times 2W}. \quad (1)$$

This dual-canvas representation forms two spatially adjacent domains—the *motion canvas* (left) and the *identity canvas* (right)—within the same latent coordinate system.

To maintain semantic separation during diffusion, we construct a binary conditioning mask

$$M_{\text{cond}} = \text{Concat}_W(\mathbf{1}_{B \times 1 \times F \times H \times W}, \mathbf{0}_{B \times 1 \times F \times H \times W}),$$

which distinguishes the editable (motion) and reference (identity) regions without constraining generation. Note that this mask is only for indication of the dual canvas, but differs from the regional mask used in the traditional inpainting which limits updates to locally masked pixels. As a result, our *mask-free* design in the whole motion canvas allows the model to learn where and how identity information should propagate. This enables extensions such as hairstyle adaptation beyond the original head boundary and improves contextual consistency around the neck and background.

For temporal coherence, we integrate motion modules from AnimateDiff [8] and train on short clips (eight frames per step), encouraging the model to maintain consistent identity and smooth dynamics over time.

4.2. Motion- and Expression-Aware Reconstruction

Standard diffusion objectives typically use a uniform Mean Squared Error (MSE) loss, assigning equal importance to all spatial regions. While this assumption is acceptable for masked or text-conditioned diffusion, it is suboptimal in our *mask-free* setting, where supervision arises solely from the input video. The model must therefore infer which regions contribute most to perceptual fidelity and temporal realism.

To address this, we propose Motion- and Expression-Aware Reconstruction (MEAR) loss, a perceptually guided loss reweighting mechanism that adaptively emphasizes motion, expression, and structural cues. As illustrated in Fig. 3, MEAR forms an attention prior by combining two complementary branches:

Motion weighting. We estimate temporal salience from inter-frame luminance differences: $D_t^{\text{raw}} = |G_{t+1} - G_t|$, where G_t is the grayscale intensity map of frame t . After dilation and normalization, we obtain a motion heatmap D that highlights dynamically changing regions.

Expression weighting. Facial expression is localized around regions such as the eyes and mouth. Using PIP-Net facial landmarks while removing boundary points, we construct a landmark response map L , perform local aggregation and Gaussian smoothing, and normalize it to form L , which softly emphasizes expression-sensitive areas.

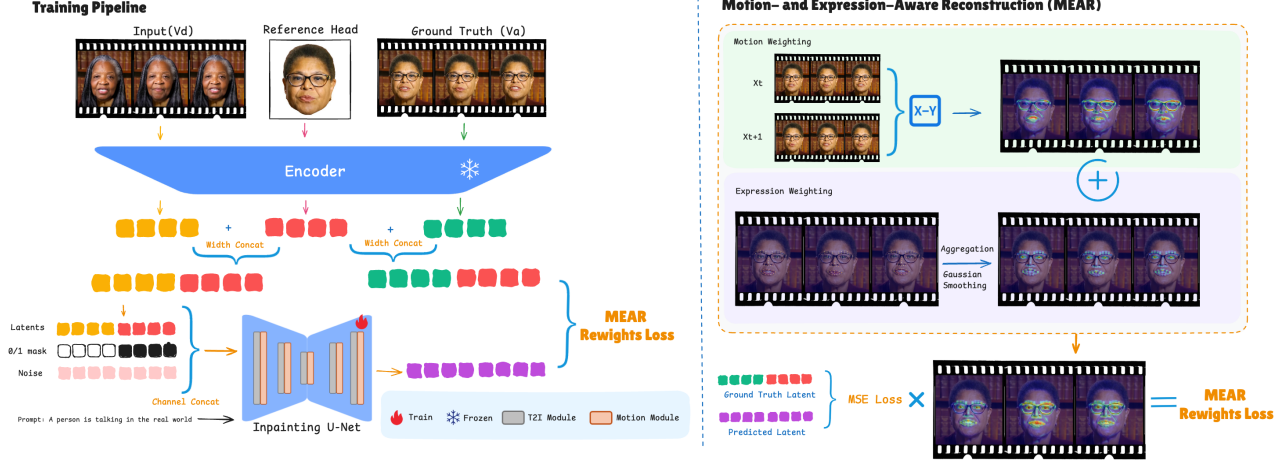


Figure 3. **Overview of the DirectSwap framework** for mask-free video head swapping. **Left:** Dual-canvas module arranges motion and identity in spatially aligned latent canvases, enabling geometry-consistent identity transport in motion enhanced U-Net model. **Right:** Motion- and Expression-Aware Reconstruction (MEAR) adaptively reweights supervision using motion and expression cues to improve perceptual fidelity and temporal coherence.

Hybrid fusion. After resizing to latent space, we unify these cues into a single prior weight:

$$A_{\text{MEAR}} = D + \alpha L(1 - D), \quad (2)$$

where α controls the balance of motion and expressive cues. This will later be used as per-pixel weights to the original MSE loss in the diffusion model. The multiplicative $(1 - D)$ acts as a soft gate, attenuating static cues in highly dynamic regions while enhancing them where motion is weak. Empirically, $\alpha = 0.5$ yields a strong trade-off between temporal smoothness and visual detail.

By combining motion and expression cues, MEAR directs the diffusion model to focus supervision on perceptually critical regions, ensuring smoother motion transitions and structurally coherent results across frames.

5. Experiments

We conduct experiments on the proposed dataset using the evaluation metrics introduced in Sec. 3, and compare our method with strong baselines, including DiffSwap [42], In-Swapper [9], IP-Adapter [38], HeadSwap [20], and VACE-Wan2.1-14B [15, 33]. We assess both quantitative and qualitative performance on the test set and in-the-wild videos. For efficiency, each video is truncated to the first 16 frames, and the reference head is extracted from the first frame. Training uses a batch size of 2 with 8-frame clips for 20,000 iterations, taking approximately 10 hours on a single NVIDIA H200 GPU. Further implementation and training details are provided in the **Supplementary Material B.1**.

5.1. Experimental Comparisons

5.2. Qualitative Results

As shown in Fig. 4, our method achieves superior identity preservation and expression transfer across frames. The first two rows are drawn from our test set, while the remaining examples depict in-the-wild scenarios.

Face-swapping approaches such as DiffSwap [42] and InSwapper [9] can replicate facial appearance but remain limited to the cropped facial region, failing to adapt head shape or hairstyle, often resulting in visible seams and geometric inconsistency (e.g., the second row). IP-Adapter [38] performs masked inpainting over the head area yet lacks explicit modeling of facial geometry. HeadSwap [20] modifies head shape but frequently compromises identity fidelity. VACE [15, 33], while text-controllable, relies on coarse masking strategies that attenuate motion and expression coherence.

In contrast, our framework synthesizes full-head results that maintain global structure, exhibit consistent identity and expressions across time, and remain robust under challenging in-the-wild conditions. Additional qualitative results are provided in the **Supplementary Material B.2**.

5.2.1. Quantitative Results

We compare our approach with five strong baselines: DiffSwap [42], InSwapper [9], IP-Adapter [38], HeadSwap [20], and VACE-Wan2.1-14B [15, 33]. 200 users rated identity preservation, expression transfer, and background blending; we report per-criterion mean opinion scores (MOS) and their average $S_{\text{average}} = \frac{S_{\text{id}} + S_{\text{expr}} + S_{\text{blend}}}{3}$ on both test data and in-the-wild videos (Tab. 1). The subjective trends are consistent with our qualitative anal-

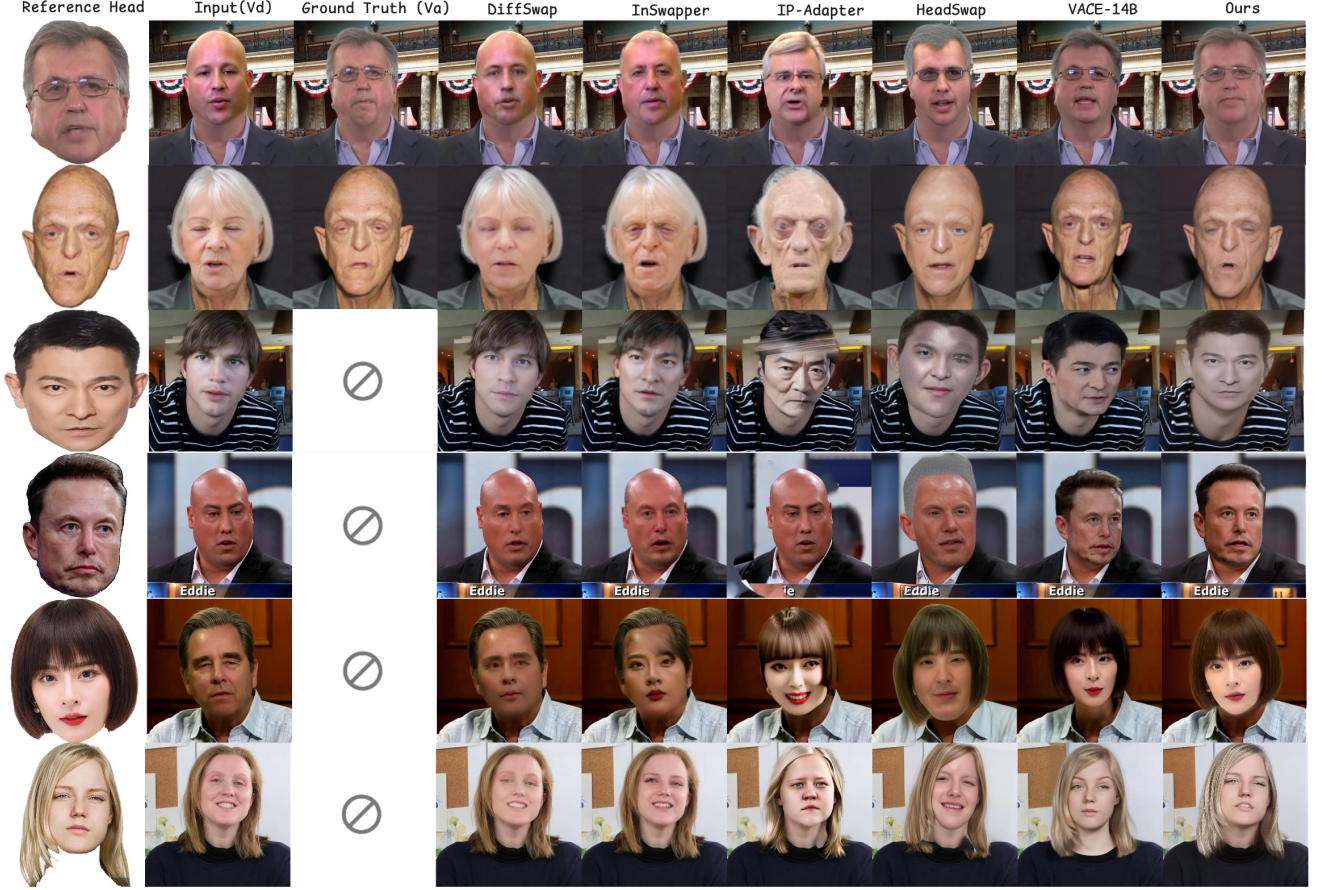


Figure 4. **Comparison with prior methods.** DiffSwap [42] and InSwapper [9] are face-swapping methods limited to the facial region, while IP-Adapter [38], HeadSwap [20], and VACE [15, 33] perform full head swapping. The first two rows show results on our test set, and the remaining rows present in-the-wild examples (where ground truth is unavailable). Our method delivers sharper geometry, stronger identity preservation, and more faithful expression transfer with superior temporal coherence.

Table 1. **User study results.** Higher is better; 100.0 is the maximum score. “Average” denotes the mean of ID, Expression, and Blend scores.

Method	ID↑	Expr.↑	Blend↑	Avg.↑
DiffSwap [42]	0.0	16.1	9.4	8.5
InSwapper [9]	0.0	41.9	9.4	17.1
IP-Adapter [38]	0.0	6.5	0.0	2.2
HeadSwap [20]	3.2	6.5	0.0	3.2
VACE [15, 33]	61.3	3.2	96.9	53.8
Ours	100.0	96.8	100.0	98.9

Table 2. **Quantitative comparison on the benchmark dataset.** Our method achieves the best overall performance across all metrics, balancing identity preservation, expression transfer, and temporal coherence. ↑ / ↓ indicate higher/lower is better.

Method	Sim _{ID} ↑	Posel↓	Expr.↓	SSIM↑	PSNR↑	LPIPS↓	FID↓	tLPIPS↓
DiffSwap [42]	0.284	2.870	0.130	0.685	15.893	0.235	40.725	0.026
InSwapper [9]	0.828	3.138	0.124	0.682	15.746	0.237	31.454	0.014
IP-Adapter [38]	0.199	4.665	0.169	0.656	15.777	0.228	27.702	0.034
HeadSwap [20]	0.357	4.047	0.141	0.662	18.245	0.196	46.877	0.045
VACE-14B [15, 33]	0.759	4.501	0.223	0.663	18.129	0.201	22.753	0.020
Ours	0.880	1.859	0.075	0.738	21.266	0.129	19.376	0.012

ysis: DiffSwap, InSwapper, IP-Adapter, and HeadSwap weaken identity preservation by either retaining the source hairstyle/head shape or distorting head geometry. Face-swapping methods (DiffSwap, InSwapper) emphasize central facial regions and thus rate higher on expression transfer, yet seams appear at facial boundaries. Rendering the

entire head together with the background, as in VACE and our method, improves transition smoothness and blending scores. Overall, our approach attains the highest S_{average} , clearly exceeding the second-best baseline (VACE).

As reported in Tab. 2, our method achieves state-of-the-art results across all metrics: highest identity similarity

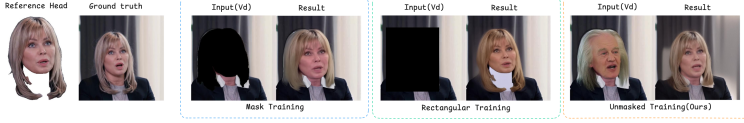


Figure 5. **Impact of training strategies.** Head masking distorts geometry, while rectangular masking weakens pose, expression, and background fidelity. Our unmasked training preserves both.



Figure 6. **Impact of Motion- and Expression-Aware Reconstruction.**

(Sim_{ID}), lowest pose and expression errors, and uniformly stronger pixel-level (SSIM/PSNR), perceptual (LPIPS), and distributional (FID) fidelity; the lowest $tLPIPS$ further indicates superior temporal stability. InSwapper’s relatively high Sim_{ID} (0.828) is expected given its reliance on ArcFace embeddings [6] during training/evaluation. VACE’s masking suppresses motion cues, degrading pose/expression fidelity and temporal smoothness; although its FID is reasonable (22.753), our approach reduces it to 19.376. Since DiffSwap and InSwapper do not modify head shape or hairstyle, and IP-Adapter and HeadSwap often lose identity fidelity, their SSIM/PSNR/LPIPS scores remain comparatively low. By jointly addressing identity, expression, and temporal coherence, our framework delivers balanced gains and consistently outperforms all baselines both quantitatively and perceptually.

5.3. Ablation Study

A common approach to video head swapping masks the head region and trains the model to inpaint the missing area using another frame as reference. However, this masking-based formulation disrupts geometric continuity and often distorts the reconstructed head. Methods such as VACE [15] employ rectangular masks, which further remove pose and expression cues and consequently produce misaligned or unnatural results. As shown in Fig. 5, head masking forces the network to reshape the synthesized head to fit the mask boundary, while rectangular masking fails to preserve pose and expression and makes background reconstruction difficult. In contrast, our unmasked formulation preserves geometric integrity and dynamic consistency, yielding realistic and temporally coherent results. Quantitative comparisons in Tab. 3 corroborate these findings: head masking lowers Sim_{ID} due to deformation, and rectangular masking

Table 3. **Training strategy comparison.** Head Mask masks the head; Rect. Mask uses a fixed rectangle.

Method	$Sim_{ID} \uparrow$	Pose \downarrow	Expr \downarrow
Head Mask	0.821	2.573	0.143
Rect. Mask	0.847	2.723	0.209
Ours	0.880	1.859	0.075

Table 4. **Effectiveness of MEAR.** Motion and expression enhance performance.

Method	$Sim_{ID} \uparrow$	Pose \downarrow	Expr \downarrow
baseline	0.871	2.182	0.082
w/o motion	0.867	2.098	0.077
w/o expression	0.873	2.019	0.080
Ours	0.880	1.859	0.075

degrades geometric and expression accuracy.

We further assess the impact of Motion- and Expression-Aware Reconstruction (MEAR) on generation quality. As shown in Fig. 6, incorporating Motion- and Expression-Aware Reconstruction markedly improves expression preservation and facial alignment. While the baseline model can capture coarse expression changes, its responses remain weak and inconsistent. Introducing only the expression cue or only the motion cue yields partial gains, but the synthesized expressions still fail to accurately follow the input. By jointly leveraging both cues, *i.e.*, landmark-based expression guidance and frame-difference motion signals, our method achieves more faithful and temporally coherent expression synthesis. Quantitative results in Tab. 4 further confirm this effect: combining expression and motion constraints improves identity similarity as well as pose and expression accuracy. Due to space limitations, we report only Sim_{ID} , pose, and expression metrics; additional ablations and results are included in the **Supplementary Material**.

6. Conclusion

We introduce HeadSwapBench, the first paired video head swapping dataset with frame-aligned identity–motion correspondences for supervised diffusion training and benchmarking. Upon this, we present DirectSwap, a mask-free direct video head swapping framework, yielding structurally natural and temporally coherent results. To further strengthen expression consistency, we propose Motion- and Expression-Aware Reconstruction (MEAR), a temporal weighted loss that extracts expression cues directly from input frames. Extensive experiments show that DirectSwap delivers high-fidelity, identity-preserving synthesis across diverse scenes and motions. More broadly, our findings suggest that unmasked, structure-aware diffusion provides a unified path towards realistic video head swapping.

References

- [1] Sanoojan Baliah, Qinliang Lin, Shengcai Liao, Xiaodan Liang, and Muhammad Haris Khan. Realistic and efficient face swapping: A unified approach with diffusion models. *arXiv preprint arXiv:2409.07269*, 2024. 1, 3
- [2] Andreas Blattmann, Robin Rombach, Huan Ling, Tim Dockhorn, Seung Wook Kim, Sanja Fidler, and Karsten Kreis. Align your latents: High-resolution video synthesis with latent diffusion models. In *Proceedings of the IEEE/CVF conference on computer vision and pattern recognition*, pages 22563–22575, 2023. 3
- [3] Xudong Cao, Yichen Wei, Fang Wen, and Jian Sun. Face alignment by explicit shape regression. *International journal of computer vision*, 107(2):177–190, 2014. 4
- [4] Renwang Chen, Xuanhong Chen, Bingbing Ni, and Yanhao Ge. Simswap: An efficient framework for high fidelity face swapping. In *Proceedings of the 28th ACM international conference on multimedia*, pages 2003–2011, 2020. 1
- [5] Ciprian Corneanu, Raghudeep Gadde, and Aleix M Martinez. Latentpaint: Image inpainting in latent space with diffusion models. In *Proceedings of the IEEE/CVF winter conference on applications of computer vision*, pages 4334–4343, 2024. 3
- [6] Jiankang Deng, Jia Guo, Niannan Xue, and Stefanos Zafeiriou. Arcface: Additive angular margin loss for deep face recognition. In *Proceedings of the IEEE/CVF conference on computer vision and pattern recognition*, pages 4690–4699, 2019. 4, 8
- [7] Gege Gao, Huaibo Huang, Chaoyou Fu, Zhaoyang Li, and Ran He. Information bottleneck disentanglement for identity swapping. In *Proceedings of the IEEE/CVF Conference on Computer Vision and Pattern Recognition (CVPR)*, pages 3404–3413, 2021. 1
- [8] Yuwei Guo, Ceyuan Yang, Anyi Rao, Zhengyang Liang, Yaohui Wang, Yu Qiao, Maneesh Agrawala, Dahua Lin, and Bo Dai. Animatediff: Animate your personalized text-to-image diffusion models without specific tuning. *arXiv preprint arXiv:2307.04725*, 2023. 3, 5
- [9] haofanwang. inswapper. <https://github.com/haofanwang/inswapper>, 2023. 6, 7
- [10] Martin Heusel, Hubert Ramsauer, Thomas Unterthiner, Bernhard Nessler, and Sepp Hochreiter. Gans trained by a two time-scale update rule converge to a local nash equilibrium. In *Advances in Neural Information Processing Systems (NeurIPS)*, pages 6626–6637, 2017. 5
- [11] Jonathan Ho, Tim Salimans, Alexey Gritsenko, William Chan, Mohammad Norouzi, and David J Fleet. Video diffusion models. *Advances in Neural Information Processing Systems*, 35:8633–8646, 2022. 3
- [12] Zheng Hui, Jie Li, Xiumei Wang, and Xinbo Gao. Image fine-grained inpainting. *arXiv preprint arXiv:2002.02609*, 2020. 3
- [13] Quan Huynh-Thu and Mohammed Ghanbari. Scope of validity of psnr in image/video quality assessment. *Electronics letters*, 44(13):800–801, 2008. 5
- [14] Chaonan Ji, Jinwei Qi, Peng Zhang, Bang Zhang, and Liefeng Bo. Controllable and expressive one-shot video head swapping. *arXiv preprint arXiv:2506.16852*, 2025. 1, 3
- [15] Zeyinzi Jiang, Zhen Han, Chaojie Mao, Jingfeng Zhang, Yulin Pan, and Yu Liu. Vace: All-in-one video creation and editing. In *Proceedings of the IEEE/CVF International Conference on Computer Vision*, pages 17191–17202, 2025. 2, 3, 4, 6, 7, 8
- [16] Haibo Jin, Shengcai Liao, and Ling Shao. Pixel-in-pixel net: Towards efficient facial landmark detection in the wild. *International Journal of Computer Vision*, 2021. 4
- [17] Taewoong Kang, Sohyun Jeong, Hyojin Jang, and Jaegul Choo. Zero-shot head swapping in real-world scenarios. *arXiv preprint arXiv:2503.00861*, 2025. 1, 3
- [18] Kihong Kim, Yunho Kim, Seokju Cho, Junyoung Seo, Jisu Nam, Kychul Lee, Seungryong Kim, and KwangHee Lee. Diffface: Diffusion-based face swapping with facial guidance. *Pattern Recognition*, 163:111451, 2025. 1, 3
- [19] Alex Krizhevsky, Ilya Sutskever, and Geoffrey E Hinton. Imagenet classification with deep convolutional neural networks. *Advances in neural information processing systems*, 25, 2012. 5
- [20] LeslieZhao. Headswap. <https://github.com/LeslieZhao/HeadSwap>, 2022. 6, 7
- [21] Hongyu Liu, Bin Jiang, Yibing Song, Wei Huang, and Chao Yang. Rethinking image inpainting via a mutual encoder-decoder with feature equalizations. In *Computer Vision—ECCV 2020: 16th European Conference, Glasgow, UK, August 23–28, 2020, Proceedings, Part II 16*, pages 725–741. Springer, 2020. 3
- [22] Camillo Lugaresi, Jiuqiang Tang, Hadon Nash, Mark McGuire, Jongmin Lee, Chuo-Ling Chang, Ming Guang Yong, Matthias Grundmann, and Vivek Kwatra. Mediapipe: A framework for building perception pipelines. *arXiv preprint arXiv:1906.08172*, 2019. 4
- [23] Andreas Lugmayr, Martin Danelljan, Andres Romero, Fisher Yu, Radu Timofte, and Luc Van Gool. Repaint: Inpainting using denoising diffusion probabilistic models. In *Proceedings of the IEEE/CVF conference on computer vision and pattern recognition*, pages 11461–11471, 2022. 3
- [24] Evangelos Ntavelis, Andrés Romero, Siavash Bigdeli, Radu Timofte, Zheng Hui, Xiumei Wang, Xinbo Gao, Chajin Shin, Taeh Kim, Hanbin Son, et al. Aim 2020 challenge on image extreme inpainting. In *Computer Vision—ECCV 2020 Workshops: Glasgow, UK, August 23–28, 2020, Proceedings, Part III 16*, pages 716–741. Springer, 2020. 3
- [25] Deepak Pathak, Philipp Krahenbuhl, Jeff Donahue, Trevor Darrell, and Alexei A Efros. Context encoders: Feature learning by inpainting. In *Proceedings of the IEEE conference on computer vision and pattern recognition*, pages 2536–2544, 2016. 3
- [26] Andreas Rossler, Davide Cozzolino, Luisa Verdoliva, Christian Riess, Justus Thies, and Matthias Nießner. Faceforensics++: Learning to detect manipulated facial images. In *Proceedings of the IEEE/CVF international conference on computer vision*, pages 1–11, 2019. 4

- [27] Changyong Shu, Hema Wu, Hang Zhou, Jiaming Liu, Zhibin Hong, Changxing Ding, Junyu Han, Jingtuo Liu, Errui Ding, and Jingdong Wang. Few-shot head swapping in the wild. In *Proceedings of the IEEE/CVF Conference on Computer Vision and Pattern Recognition*, pages 10789–10798, 2022. 1, 3
- [28] Aliaksandr Siarohin, Stéphane Lathuilière, Sergey Tulyakov, Elisa Ricci, and Nicu Sebe. First order motion model for image animation. *Advances in neural information processing systems*, 32, 2019. 5
- [29] Jascha Sohl-Dickstein, Eric Weiss, Niru Maheswaranathan, and Surya Ganguli. Deep unsupervised learning using nonequilibrium thermodynamics. In *International conference on machine learning*, pages 2256–2265. pmlr, 2015. 3
- [30] Yang Song, Jascha Sohl-Dickstein, Diederik P Kingma, Abhishek Kumar, Stefano Ermon, and Ben Poole. Score-based generative modeling through stochastic differential equations. *arXiv preprint arXiv:2011.13456*, 2020. 3
- [31] Christian Szegedy, Vincent Vanhoucke, Sergey Ioffe, Jon Shlens, and Zbigniew Wojna. Rethinking the inception architecture for computer vision. In *Proceedings of the IEEE conference on computer vision and pattern recognition*, pages 2818–2826, 2016. 5
- [32] Qwen Team. Qwen2.5-vl, 2025. 4
- [33] Ang Wang, Baole Ai, Bin Wen, Chaojie Mao, Chen-Wei Xie, Di Chen, Feiwu Yu, Haiming Zhao, Jianxiao Yang, Jianyuan Zeng, Jiayu Wang, Jingfeng Zhang, Jingren Zhou, Jinkai Wang, Jixuan Chen, Kai Zhu, Kang Zhao, Keyu Yan, Lianghua Huang, Mengyang Feng, Ningyi Zhang, Pandeng Li, Pingyu Wu, Ruihang Chu, Ruili Feng, Shiwei Zhang, Siyang Sun, Tao Fang, Tianxing Wang, Tianyi Gui, Tingyu Weng, Tong Shen, Wei Lin, Wei Wang, Wei Wang, Wenmeng Zhou, Wenten Wang, Wenting Shen, Wenyuan Yu, Xianzhong Shi, Xiaoming Huang, Xin Xu, Yan Kou, Yangyu Lv, Yifei Li, Yijing Liu, Yiming Wang, Yingya Zhang, Yitong Huang, Yong Li, You Wu, Yu Liu, Yulin Pan, Yun Zheng, Yuntao Hong, Yupeng Shi, Yutong Feng, Zeyinzi Jiang, Zhen Han, Zhi-Fan Wu, and Ziyu Liu. Wan: Open and advanced large-scale video generative models. *arXiv preprint arXiv:2503.20314*, 2025. 6, 7
- [34] Qinghe Wang, Lijie Liu, Miao Hua, Pengfei Zhu, Wangmeng Zuo, Qinghua Hu, Huchuan Lu, and Bing Cao. Hs-diffusion: Semantic-mixing diffusion for head swapping. *arXiv preprint arXiv:2212.06458*, 2022. 1, 3
- [35] Zhou Wang, Alan C Bovik, Hamid R Sheikh, and Eero P Simoncelli. Image quality assessment: from error visibility to structural similarity. *IEEE transactions on image processing*, 13(4):600–612, 2004. 5
- [36] Cho-Ying Wu, Qiangeng Xu, and Ulrich Neumann. Synergy between 3dmm and 3d landmarks for accurate 3d facial geometry. In *2021 International Conference on 3D Vision (3DV)*, 2021. 5
- [37] Liangbin Xie, Xintao Wang, Honglun Zhang, Chao Dong, and Ying Shan. Vfhq: A high-quality dataset and benchmark for video face super-resolution. In *The IEEE Conference on Computer Vision and Pattern Recognition Workshops (CVPRW)*, 2022. 3
- [38] Hu Ye, Jun Zhang, Sibor Liu, Xiao Han, and Wei Yang. Ip-adapt: Text compatible image prompt adapter for text-to-image diffusion models. *arXiv preprint arxiv:2308.06721*, 2023. 6, 7
- [39] David Junhao Zhang, Jay Zhangjie Wu, Jia-Wei Liu, Rui Zhao, Lingmin Ran, Yuchao Gu, Difei Gao, and Mike Zheng Shou. Show-1: Marrying pixel and latent diffusion models for text-to-video generation. *International Journal of Computer Vision*, pages 1–15, 2024. 3
- [40] Richard Zhang, Phillip Isola, Alexei A Efros, Eli Shechtman, and Oliver Wang. The unreasonable effectiveness of deep features as a perceptual metric. In *Proceedings of the IEEE conference on computer vision and pattern recognition*, pages 586–595, 2018. 5
- [41] Zhimeng Zhang, Lincheng Li, Yu Ding, and Changjie Fan. Flow-guided one-shot talking face generation with a high-resolution audio-visual dataset. In *Proceedings of the IEEE/CVF Conference on Computer Vision and Pattern Recognition*, pages 3661–3670, 2021. 3
- [42] Wenliang Zhao, Yongming Rao, Weikang Shi, Zuyan Liu, Jie Zhou, and Jiwen Lu. Diffswap: High-fidelity and controllable face swapping via 3d-aware masked diffusion. *CVPR*, 2023. 1, 3, 6, 7